Nonlinear Horizontal Site Amplification for Constraining the NGA-West2 GMPEs

Ronnie Kamai,[a] M.EERI, **Norman A. Abrahamson,**[b] M.EERI, **and Walter J. Silva,**[c] M.EERI

The nonlinear soil amplification models developed by Walling et al. (2008) are revisited for three main reasons: (a) the simulation database on which the models were developed has been updated and extended, (b) two alternatives for the input shaking parameter—(PGA and $Sa(T)$)—are explored, and (c) a constraint on the nonlinearity at long periods is removed. The model is based on site amplification factors, relative to a $V_{S30} = 1{,}180$ m/s site. Simulations included a wide range of soil profiles, shaking amplitudes and soil properties, from which only a subset was used herein. Finally, four models for the nonlinear site amplification are developed using two nonlinear material property models (peninsular range and EPRI) and two input-shaking parameters (PGA_{1180} and $Sa_{1180}(T)$). These results are intended for use by the NGA-West2 developers to constrain the nonlinear scaling of the site response for the horizontal ground motion models. [DOI: 10.1193/070113EQS187M]

INTRODUCTION

The purpose of this work is to provide the developers of the ground motion prediction equations (GMPE) in the NGA-West2 project with a model that describes the nonlinear response of soil sites within the NGA-West2 ground motion database. This model is not intended to be used for site-specific response analysis applications, but rather to allow soil sites to be incorporated into the derivation of the GMPE so that nonlinear soil effects are not mapped into the magnitude or distance scaling. The alternative, for a developer who chooses not to include nonlinear effects in their GMPE, is to eliminate all soil data, which greatly reduces the amount of data used at close distances from large earthquakes.

Nonlinear site response was incorporated into four out of the five ground motion prediction equations (GMPEs) developed as part of the first Next Generation Attenuation (NGA) project in 2008 (Abrahamson et al. 2008). The nonlinear scaling of the site response was constrained by empirical data in two of the GPMEs (Boore and Atkinson 2008, Chiou and Youngs 2008), and by numerical simulations in the other two (Abrahamson and Silva 2008, Campbell and Bozorgnia 2008). The new NGA-West2 data set described in Ancheta et al. (2014) has been significantly extended compared to the 2008 data set described in Chiou et al. (2008), with the 2014 data set including many more recordings and a significantly improved representation of both soft soil sites and hard rock sites. Figure 1

[a] Ben Gurion University of the Negev, Israel, 84105
[b] Pacific Gas and Electric Company, 245 Market St., San Francisco, CA 94105
[c] Pacific Engineering and Analysis, 311 Pomona Ave., El Cerrito, CA 94546

Earthquake Spectra, Volume 30, No. 3, pages 1223–1240, August 2014;

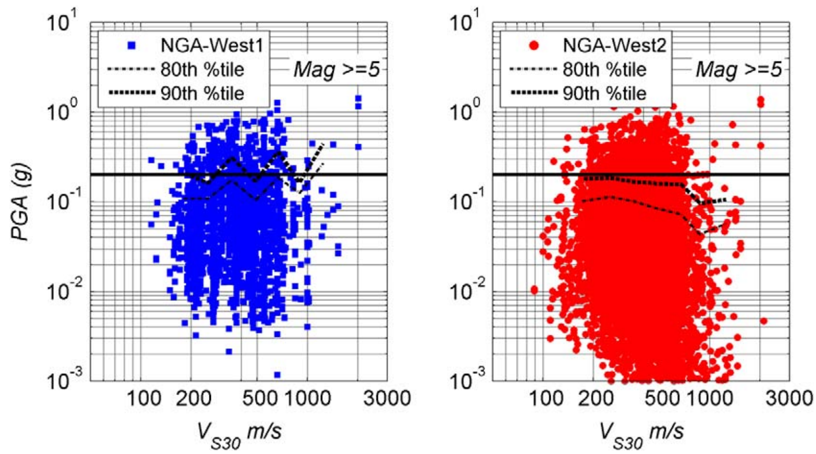

Figure 1. Distribution of PGA and V_{S30} in the two NGA databases in the magnitude range of $\mathbf{M} \geq 5.5$. The 90th percentile of each bin is shown by the dashed line, while an approximate nonlinear threshold is shown by a black line at PGA = 0.2 g.

compares the distributions of the peak ground acceleration (PGA) and the shear-wave velocity over the top 30 m (V_{S30}) for the 2008 and 2014 data sets for $\mathbf{M} \geq 5$. The two dashed lines represent the 80th and 90th percentiles of the data (binned into seven V_{S30} bins), while the solid line represents PGA = 0.2 g, which is approximately the lower limit for significant nonlinear effects. As seen in Figure 1, although the 2014 data set contains almost twice as many recordings in the nonlinear range when compared to the 2008 data set (623 in 2014 versus 313 in 2008), the sampling of ground motions for which nonlinear site response effects would be strong remains sparse, and most of the recorded data are well below a PGA of 0.2 g.

Due to the scarcity of data in the high ground motion ranges required to constrain the nonlinear site response, analytical models based on one-dimensional (1-D) site response simulations are used to provide guidance on the extrapolation of the nonlinear site factors in the GMPEs where data is still lacking. While the simulations used to develop the models presented herein use the same site response methodology as in Walling et al. (2008), the number and range of scenarios has been extended: Instead of using only one magnitude ($\mathbf{M}$ 6.5), the simulations used in this study included three different magnitudes: $\mathbf{M}$ 5.0, $\mathbf{M}$ 6.0, and $\mathbf{M}$ 7.0. In addition, a profile with a lower shear-wave velocity ($V_{S30} = 190$ m/s) was added to extend the analytical results to softer profiles.

Nonlinearity in the soil response to ground motion is typically considered to be related to the intensity of the input ground motion on a nearby rock outcrop. The reference rock ground motion can be parameterized by its magnitude, distance from source, PGA, spectral acceleration ($Sa(T)$), or any combination of the above. Bazzurro and Cornell (2004) conducted a numerical site response study on two soil profiles, subjecting them to 78 input ground motions and exploring seven different approaches to modeling the nonlinear site amplification. They concluded that the spectral acceleration for the reference rock motion, $Sa_{Ref}(T)$, is the most efficient single parameter to describe the input motion for estimating the nonlinear site amplification at spectral period T. Chiou and Youngs (2008) followed that approach and used $Sa_{Ref}(T)$ as the strength of shaking parameter in their site amplification function. In the Walling et al. (2008) model, used by Abrahamson and Silva (2008) and by Campbell and Bozorgnia (2008), the strength of shaking is defined in terms of the PGA on a reference site, PGA_{Ref}. PGA has been widely used by the geotechnical community to define the level of shaking for nonlinear effects because it is related to the peak stress and hence controls the amount of strain within the soil profile, which determines the nonlinear response. However, PGA_{Ref} is strongly correlated with $Sa_{Ref}(T)$, especially in the site response method used to define the input rock motion in Walling et al. (2008) and in this study, so there is not a large difference between the resulting models. Using the spectral acceleration at the period of interest simplifies the application of the models because it does not require the correlation of the PGA and $Sa(T)$ variability to be tracked as part of the standard deviation (e.g., Al Atik and Abrahamson 2010). In this paper, we present nonlinear site models for both of these approaches for parameterizing the level of shaking: one with PGA_{Ref} and one with $Sa_{Ref}(T)$ as the input motion.

SITE RESPONSE SIMULATIONS

The site response calculations are conducted using the computer program RASCALS (Silva and Lee 1987). The RASCALS program combines the single-corner point-source model for the Fourier amplitude spectrum, commonly used in seismology to define the source and path scaling of earthquakes, with the equivalent-linear site response approach response, commonly used in geotechnical engineering to estimate the nonlinear behavior of soils. The complete set of simulations, including theory, background, and example results, is described in Kamai et al. (2013). Only the subsets that were used to develop the parametric models presented herein are described below.

Three earthquakes, with **M** 5.0, **M** 6.0, and **M** 7.0 and a constant stress drop of 50 bars, are used to define the seismic source for the reference outcrop motion. Each input motion is first propagated through a profile with $V_{S30} = 1{,}180$ m/s, using the 1-D SH site response method. Eleven levels of PGA for a V_{S30} of 1,180 m/s (PGA_{1180}) are considered: 0.01 g, 0.05 g, 0.1 g, 0.2 g, 0.3 g, 0.4 g, 0.5 g, 0.75 g, 1.0 g, 1.25 g, and 1.5 g. The distance for the point-source model is adjusted so that the PGA for the reference rock profile ($V_{S30} = 1{,}180$ m/s) matches the desired target PGA_{1180} value. For each combination of magnitude and PGA_{1180}, the point-source distance is kept fixed, and the top 30–1,000 ft of the velocity profile are replaced to represent a soil profile (defined by both V_{S30} and the depth to $V_S = 1{,}000$ m/s). To obtain consistent kappa values on both rock and soil sites, as observed in California data, the kappa for the input rock motion (e.g., the kappa used in the point-source model) was reduced so that the total kappa for a 1,000 ft profile would remain at 0.04 s, consistent with observations. Specific values for each profile are given in Kamai et al. (2013). The amplification factors for each case are computed as the ratio between the 5% damped spectral acceleration from the surface motion using the soil profile to that of the corresponding reference rock ($V_{S30} = 1{,}180$ m/s) outcrop.

The base soil profiles include six V_{S30} values (190 m/s, 270 m/s, 400 m/s, 560 m/s, 760 m/s, and 900 m/s), with a randomized depth to bedrock, defined as depth to

$V_S = 1{,}000$ m/s (called Z_1 in the GMPEs; see Table 1). The nonlinear soil response is characterized by the strain dependence of the G/G_{max} and hysteretic damping, for which two models are used: EPRI (1993) and peninsular range, called here PR for brevity (see Walling et al. 2008 and Kamai et al. 2013 for soil curves and shear wave velocity profiles).

For each combination of base soil profile, input PGA (PGA_{1180}), and point-source magnitude, 30 realizations were computed, randomizing the shear-wave velocity profile, layer thickness, and nonlinear soil properties (strain dependence of the G/G_{max} and hysteretic damping). The algorithm starts with a given base-case profile and generates a suite of random profiles about the base-case profile accounting for correlation of the velocities and layer thickness variations. An example for 30 random profiles with an average V_{S30} of 270 m/s is given in Figure 2. The details of the procedure are summarized in Kamai et al. (2013) and provided with more detail in Silva et al. (1996).

PARAMETRIC MODEL FOR NONLINEAR SITE AMPLIFICATION

The simulation cases described above were used for the development of parametric models for the nonlinear response of soil sites to strong ground motions. The proposed models are updates to the models developed by Walling et al. (2008) and use the same functional form.

While the reference velocity in Walling et al. (2008), followed by Abrahamson and Silva (2008) and Campbell and Bozorgnia (2008), was defined as 1,100 m/s, we redefine the V_{S30} of the reference profile as 1,180 m/s, which is more accurate with respect to the values used in the simulations. However, the effect on the nonlinear term is insignificant.

Four resulting models are presented below, based on two material property models, PR and EPRI, and on two parameters for the level of shaking, PGA_{1180} and $Sa_{1180}(T)$. The PR models are applicable for V_{S30} from 190–900 m/s, whereas the EPRI models are applicable for V_{S30} from 270–900 m/s. A summary of the simulation cases used for model development is presented in Table 1.

PERIOD RANGE

The random vibration theory (RVT) method becomes inapplicable when the oscillator period (corresponding to the spectral period) exceeds the corner period of the source. This led to an unrealistic shape of the amplification vs. period at long periods, as further discussed in

Table 1. List of simulation scenarios that were selected for model development

V_{S30} (m/s)	Depth to top of rock ($V_S = 1$ km/s)	Material model used for nonlinear properties
190	9–305 m	PR
270	9–305 m	PR, EPRI
400	9–305 m	PR, EPRI
560	9–305 m	PR, EPRI
760	79 m	PR, EPRI
900	79 m	PR

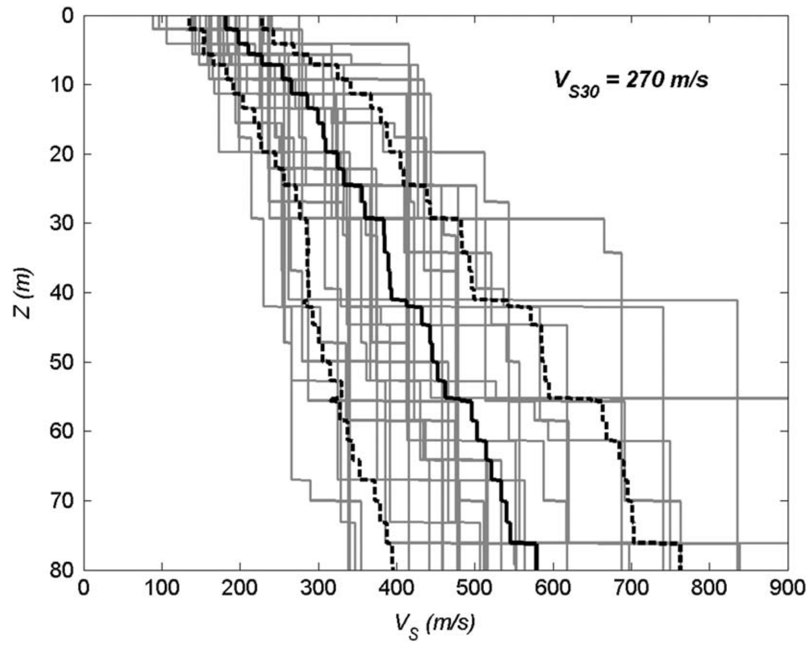

Figure 2. Thirty random shear wave velocity profiles with an average V_{S30} of 270 m/s. The black lines represent the mean and ± 1 standard deviation of the V_S at any given depth.

Kamai et al. (2013). To address this shortcoming, a magnitude-period constraint was placed on the data set used for the regression analysis. The simulation results used for model regression include the **M** 7.0 simulations within the entire available period range $0.01\ \mathrm{s} < T < 10\ \mathrm{s}$, **M** 6.0 simulations at $0.01\ \mathrm{s} < T < 5\ \mathrm{s}$ and **M** 5.0 simulations at $0.01\ \mathrm{s} < T < 2\ \mathrm{s}$.

FUNCTIONAL FORM

The functional form is identical to that used in Walling et al. (2008). It can be written as the sum of a linear term and a nonlinear term:

$$\ln(Amp) = f_L(V_{S30}) + f_{NL}(GM_{Ref}, V_{S30}) \tag{1}$$

The linear term is a function of V_{S30} only, whereas the nonlinear term is a function of V_{S30} and a measure of the shaking intensity on a reference site, here defined as $V_{S30} = 1{,}180$ m/s. The resulting functional forms for the two alternative models are given in Equations 2 and 3 for the PGA-based and the $Sa(T)$-based models, respectively:

$$\ln(Amp) = \begin{cases} a\ ln\left(\frac{V_{S30}^*}{V_{Lin}}\right) - b\ ln(PGA_{1180} + c) \\ +b\ ln\left(PGA_{1180} + c\left(\frac{V_{S30}^*}{V_{Lin}}\right)^n\right) + d & for\ V_{S30} < V_{Lin} \\ (a + bn)\ ln\left(\frac{V_{S30}^*}{V_{Lin}}\right) + d & for\ V_{S30} \geq V_{Lin} \end{cases} \tag{2}$$

$$\ln(Amp) = \begin{cases} a\ ln\left(\frac{V^*_{S30}}{V_{Lin}}\right) - b\ ln(Sa_{1180}(T) + c) \\ +b\ ln\left(Sa_{1180}(T) + c\left(\frac{V^*_{S30}}{V_{Lin}}\right)^n\right) + d & for\ V_{S30} < V_{Lin} \\ (a + bn)\ ln\left(\frac{V^*_{S30}}{V_{Lin}}\right) + d & for\ V_{S30} \geq V_{Lin} \end{cases} \tag{3}$$

where

$$V^*_{S30} = \begin{cases} V_{S30} & for\ V_{S30} < V_1 \\ V_1 & for\ V_{S30} \geq V_1 \end{cases} \tag{4}$$

In Equations 2–4, a, b, c, d, and n are model parameters which are derived through a regression analysis. V_{Lin} represents the shear wave velocity above which the site response is linear and V_1 corresponds to the shear wave velocity above which the soil amplification is no longer correlated with changes in V_{S30}. While V_{Lin} is derived through the regression analysis and is directly related to the specific nonlinear model, V_1 is derived empirically and is related to the empirical database and the corresponding GMPE. The derivation of V_1 is explained in Abrahamson and Silva (2008) and in Abrahamson et al. (2013).

MODEL PARAMETERS

The parameters b, n, and c, which appear in the nonlinear term in Equations 2 and 3 are highly correlated. Therefore, as a first step, the parameters n and c were fixed to a constant value across all periods. Fixing the n and c coefficients was done based on regressions of smaller subsets at short periods, where the nonlinearity is strongest. The fixed values for n and c are given in Table 2. In the second step, V_{Lin} was estimated, and a smoothed period-dependent V_{Lin} was developed. In the third step, the n, c, and V_{Lin} terms were held fixed, and the period-dependent nonlinear coefficient, b, was estimated and smoothed.

Smoothing of the period-dependent parameters was done by fitting a seventh-order polynomial to the regressed values with some constraints at the low and high ends of the period range, following Equation 5.

$$x = \begin{cases} \beta_2 & T \geq T_2 \\ \alpha_0 + \sum_{i=1}^{7} \alpha_i [ln(T/T_0)]^i & T_1 < T < T_2 \\ \beta_1 & T \leq T_1 \end{cases} \tag{5}$$

The smoothed parameter x in Equation 5 is either $ln\,(V_{Lin})$ or b, and T is the spectral period. The parameters needed for computing the nonlinear terms (following Equation 5) are presented in Table 2. The smoothed values for V_{Lin} and b are shown in Figure 3 and are listed in the Electronic Supplement for the 111 periods that are in the NGA Database flatfile. The remaining parameters are left unsmoothed because they are not needed to constrain the nonlinear site response and they are correlated with other terms in the GMPE. For example, a in our model describes the scaling of linear soil amplification and is derived empirically for each GMPE separately. The parameter d in our model is a constant that adjusts the amplification if the reference conditions are different than $V_{S30} = 1{,}180$ m/s.

Table 2. List of coefficients for use in Equations 2 and 3 to compute the median nonlinear soil amplification for four cases

	PR			EPRI		
		PGA	Sa		PGA	Sa
	n	1.5	1.5		1.5	1.5
	c	1.4	2.4 (×100 for PGV)		2.0	3.0 (×100 for PGV)
	V_{Lin}	b	b	V_{Lin}	b	b
PGV	332.00	−1.5140	−2.0200	728.00	0.5850	0.6025
T_0	0.010	0.020	0.012	0.014	0.010	0.02
T_1	0.015	0.020	0.018	0.018	0.022	0.018
T_2	0.550	9.000	5.500	0.460	1.820	7.000
α_0	6.5300	−1.2500	−1.6400	7.1360	−0.9039	−0.9241
α_1	−0.2000	0.2780	0.9474	−0.6500	1.1276	0.3081
α_2	0.2400	−1.3430	−2.0673	1.7860	−3.5267	0.2166
α_3	0.0940	2.4810	2.2630	−1.0370	4.4341	−0.5068
α_4	−0.0170	−1.8690	−1.0634	0.1237	−2.5880	0.1586
α_5	−0.0529	0.6040	0.2097	0.0421	0.7361	0.0006
α_6	0.0191	−0.0862	−0.0155	−0.0117	−0.0993	−0.0047
α_7	−0.0018	0.0045	0.0002	0.0008	0.0051	0.0004
β_1	6.493	−1.250	−1.470	7.068	−0.833	−0.960
β_2	5.805	0.360	3.950	6.590	0.600	2.100

Note that while the parameter b was constrained in Walling et al. (2008) to be mostly negative (or <0.15), it was allowed to be positive without constraint in the models developed in this paper. The positive b values allow an increase in amplification for increased levels of shaking, which is a result of period elongation.

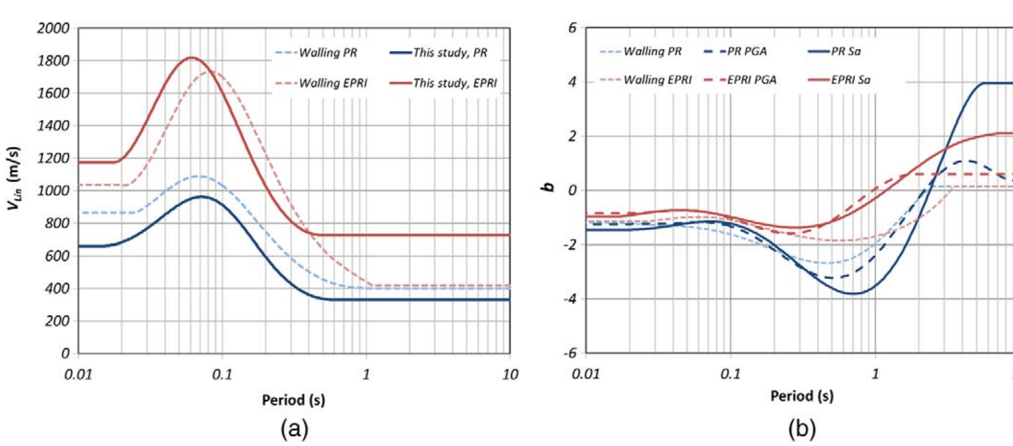

Figure 3. Period-dependence of the smoothed model parameters (a) V_{Lin} and (b) b.

RESULTS AND DISCUSSION

MODELS VERSUS SIMULATION RESULTS

The site amplification as a function of shaking intensity and soil profile (parameterized in terms of V_{S30}) is presented in Figure 4 for the PR-Sa model only, for periods 0.01 s, 0.2 s, 1 s, 2 s, 3 s, and 5 s (similar figures for the three other models can be found in Kamai et al. 2013). The median simulation results are represented by open symbols while the parametric model is shown by the solid line for each corresponding V_{S30}. The example in Figure 4 shows that the parametric form generally captures the trends from the simulations. At low shaking intensities (the linear range), the log amplification is inversely proportional to log V_{S30}—as the profile is softer, it has stronger linear amplification. As input shaking levels increase, the amplification at short periods decreases as a manifestation of increased damping. At long periods, the amplification is not dependent on shaking intensity for the stiffer profiles,

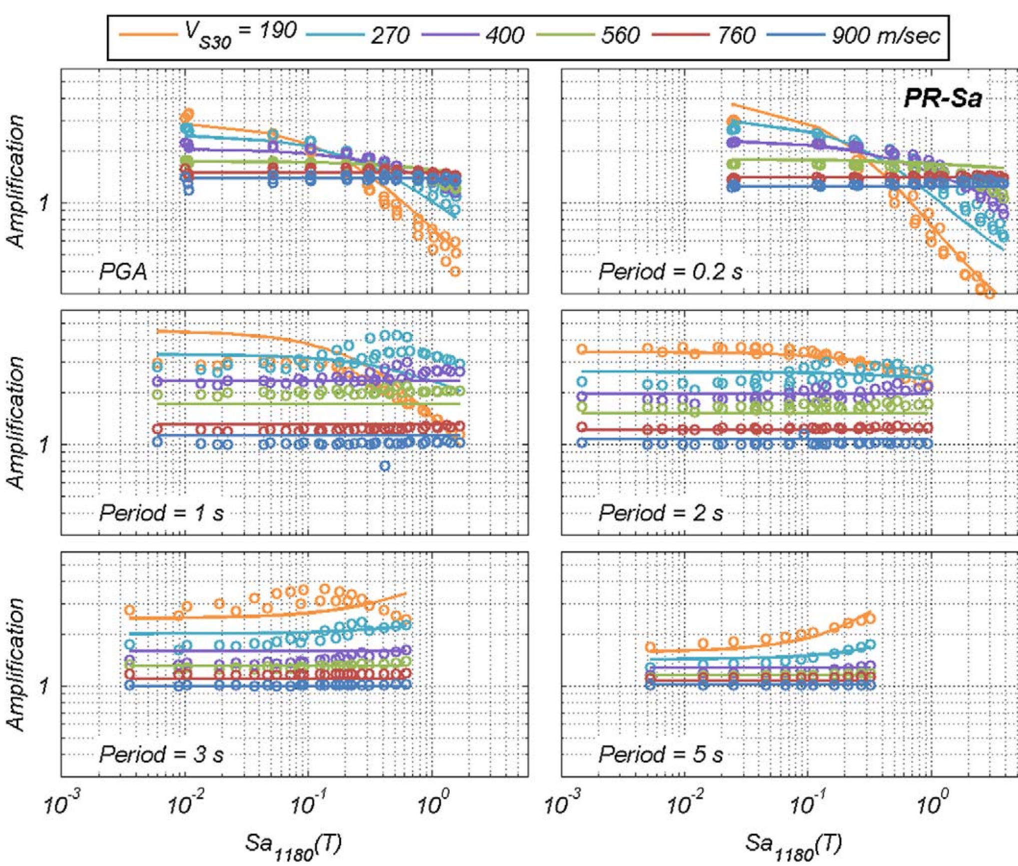

Figure 4. Comparison of the site amplification from the parametric model given in Equation 3 (solid lines) with the median site amplification from the simulations averaged over the 30 profile randomizations, for the PR-Sa model for six representative periods.

but increases with shaking for the softer profiles. This increased amplification with shaking is a result of the peak of the spectra shifting to longer periods as the soil profile becomes softer, as will be shown below.

The main discrepancy between the smooth parametric model and the simulation data-points appears at around $T = 1$ s and $T = 3$ s for the profiles with $V_{S30} = 270$ m/s and 190 m/s, respectively. This discrepancy results from several aspects of the soil response that cannot be captured by the simple functional form shown in equations 2 and 3. For example, in Figure 4 at $T = 1$ s, the simulations for $V_{S30} = 190$ m/s display the typical downward trend, while the simulations for $V_{S30} = 270$ m/s peak at around $PGA_{1180} = 0.5$ g, after which there is a decrease in amplification. The current functional form of the model cannot capture an increase followed by a decrease in amplification since the single parameter b controls the shape of the curve. A positive value of b will result in an upward curve, and a negative b will result in a downward curve at that period, for all V_{S30} values. Therefore, b is chosen by the regression such that it minimizes the error for all profiles, resulting in a misfit, which is clearly seen at $T = 1$ s, for the $V_{S30} = 270$ profile at stronger shaking. This could affect the nonlinear scaling for $V_{S30} < 300$ m/s for periods near 1 s. In addition, the current functional form constrains the linear amplification (amplification at low levels of input shaking) to scale linearly with V_{S30}. This is a simplifying assumption, as observed by the nearly identical amplification of the simulation data points for $V_{S30} = 190$ m/s and $V_{S30} = 270$ m/s profiles at low shaking intensities at $T = 0.2$ and 1 s (i.e., no V_{S30} scaling in that range of V_{S30} and T). Using a higher-order polynomial to describe the V_{S30} scaling at low shaking intensities may capture this effect. However, since our goal is to describe the nonlinear term, these refinements of the linear model are not significant for our objective.

The scatter of the simulation data-points (e.g., Figure 4, $V_{S30} = 190$ m/s, $PGA_{Ref} = 1.5$ g) is due to the different earthquake magnitudes and is mostly evident at strong shaking intensities. Generally, for the simulation results discussed here, the amplification is proportional to magnitude at short periods and inversely proportional to magnitude at long periods, which is consistent with the results from Zhao et al. (2009). However, we only find a significant magnitude dependence for soft profiles and at strong shaking intensities ($PGA_{1180} \geq 0.5$ g) or around the resonance peak (typically $T = 1$ s). Hence, this scatter does not appear significant enough to justify adding additional complexity to our functional form to account for magnitude dependence.

SOIL RESPONSE

The average spectral acceleration of the soil, given the input spectral acceleration on the reference rock and the corresponding model amplification can be computed as:

$$Sa_{soil}(T, V_{S30}) = Sa_{Ref}(T) \cdot Amp(T, V_{S30}) \tag{6}$$

The spectral shape of the rock and corresponding soil motions are presented in Figure 5 for four increasing shaking intensities, ranging from PGA_{1180} of 0.05 g to 1 g. The rock motions are shown in solid lines and the corresponding soil motions are in dashed lines. It can be seen that as shaking increases and the soil profiles is under higher strains, stiffness decreases and peak response is shifted towards longer periods. This period elongation is

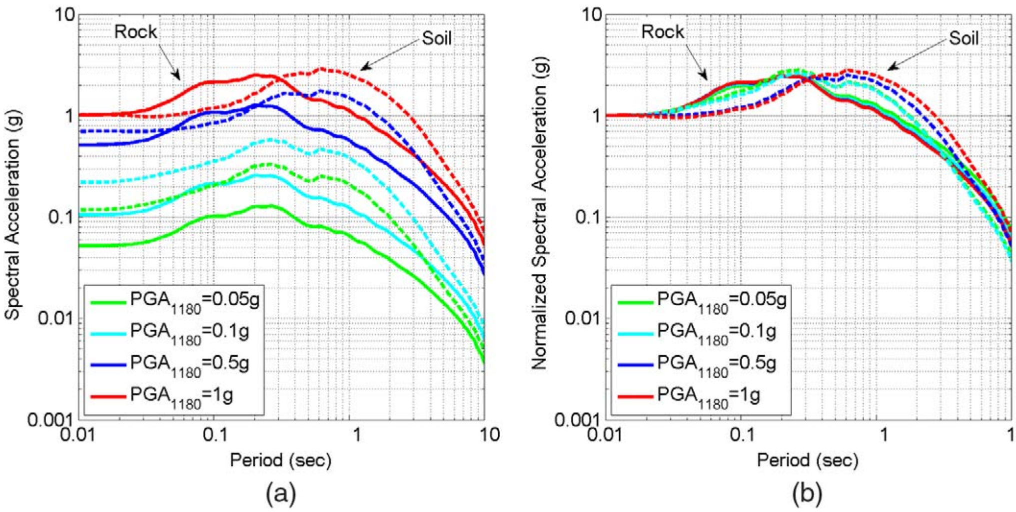

Figure 5. (a) Spectral acceleration and (b) normalized spectral acceleration versus period, for the PR-Sa model with $V_{S30} = 270$ m/s and under four different input shaking intensities.

typical of soil profiles under strong shaking and can explain the upward trend of the amplification curve at longer periods in Figure 4.

The four amplification models are compared in Figure 6 in terms of their resulting soil spectral shape for $V_{S30} = 270$ m/s with (a) $PGA_{1180} = 0.1$ g and (b) $PGA_{1180} = 0.5$ g. It can

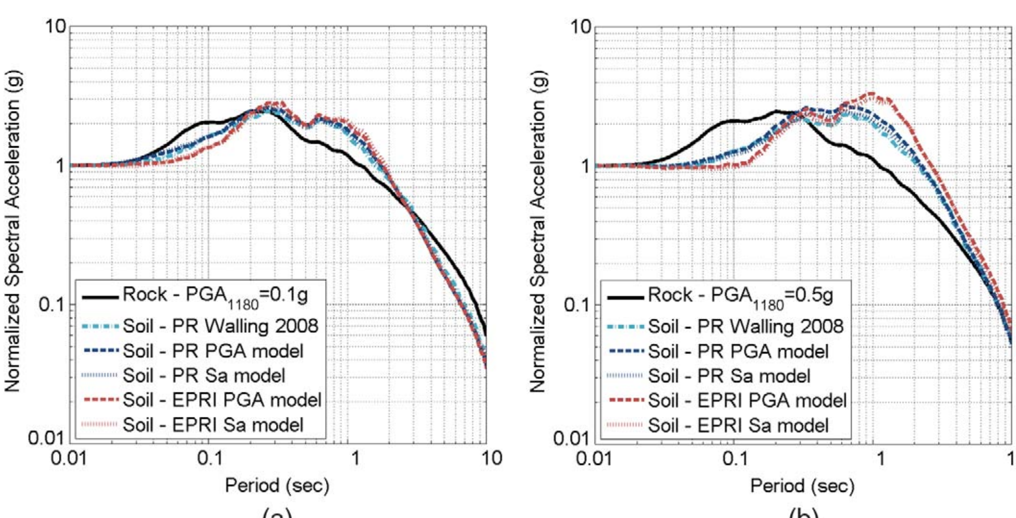

Figure 6. Normalized spectral acceleration vs. Period for a $V_{S30} = 270$ m/s profile with (a) $PGA_{1180} = 0.1$ g and (b) $PGA_{1180} = 0.5$ g.

be seen that while all four models result in a largely similar soil spectra, there is a greater difference between the two nonlinear material models (i.e., PR versus EPRI) than between the two forms of the input motion (i.e., PGA versus $Sa(T)$). For comparison, the PR model from Walling et al. (2008) is also presented on Figure 6. For the conditions shown in Figure 6 it is very similar to the current PR-PGA model.

NONLINEARITY

A comparison between the four new models and other implementations of nonlinearity into NGA GMPEs is presented in Figure 7, in terms of the normalized amplification as a function of the level of shaking. The new models are compared with nonlinear models from NGA-West1 and NGA-West2 in Figure 7a and 7b, respectively. The reference site conditions are all adjusted to represent a site with $V_{S30} = 760$ m/s. To obtain $Sa(T)_{Ref}$ for the models that require $Sa(T)$ as input (CY08, CY14, PR-Sa, and EPRI-Sa), the input PGA is first multiplied by a reference spectral shape, corresponding to a reverse event with **M** 7.5, $R_{JB} = 0$, and $V_{S30} = 1{,}130$ m/s and then adjusted to PGA_{760} for plotting purposes. The normalized amplification was obtained by computing the difference in amplification between a soil profile with $V_{S30} = 270$ m/s to a profile with $V_{S30} = 760$ m/s. The amplification is then normalized by the amplification ratio at $PGA_{760} = 0.01$ g, so that the comparison is done for the nonlinear term only.

There are three approaches for treatment of nonlinear soil response in the NGA GMPE's: to use simulation results to constrain the response, to use data regression to constrain the response, or to not include nonlinearity at all. The simulation-driven nonlinear implementations include Abrahamson and Silva (2008; denoted here as AS08), Campbell and Bozorgnia (2008; denoted here as CB08), Abrahamson et al. (2014; denoted here as ASK14), and Campbell and Bozorgnia (2014; denoted here CB14). While AS08, CB08, and CB14 use the PR-based model from Walling et al. (2008; denoted here W08-PR), ASK14 updated their nonlinear term to use the PR-Sa model presented herein. The data-driven nonlinear implementations include Chiou and Youngs (2008, 2014; denoted here CY08 and CY14, respectively), who used a functional form constrained by the Walling et al. (2008) models but determined the amount of nonlinearity based on their empirical regression. Boore and Atkinson (2008; denoted here BA08) used a simplified version of the Choi and Stewart (2005) nonlinear model, constrained by empirical data. Their successor GMPE, Boore et al. (2014; denoted here BSSA14) used a model developed by Seyhan and Stewart (2014), who compared the levels of nonlinearity from the simulations with parameterized values from data and built a model that considers both sources. Finally, Idriss (2008, 2014) does not consider nonlinearity in his GMPE and instead limits the range of applicable V_{S30} in his model.

Generally speaking, nonlinearity of the simulation-driven models (e.g., ASK14 and CB14) is greater than that of the data-driven models (e.g., BSSA14 and CY14) and leads to a "steeper" amplification slope. While the available data shows less nonlinearity than the simulations, data in the nonlinear range is quite limited (see Figure 1). This source of epistemic uncertainty is also discussed by Seyhan and Stewart (2014). While the new models are generally consistent with the Walling et al. (2008) models (as expected, being based on the same simulation methodology), they are more nonlinear at mid-periods,

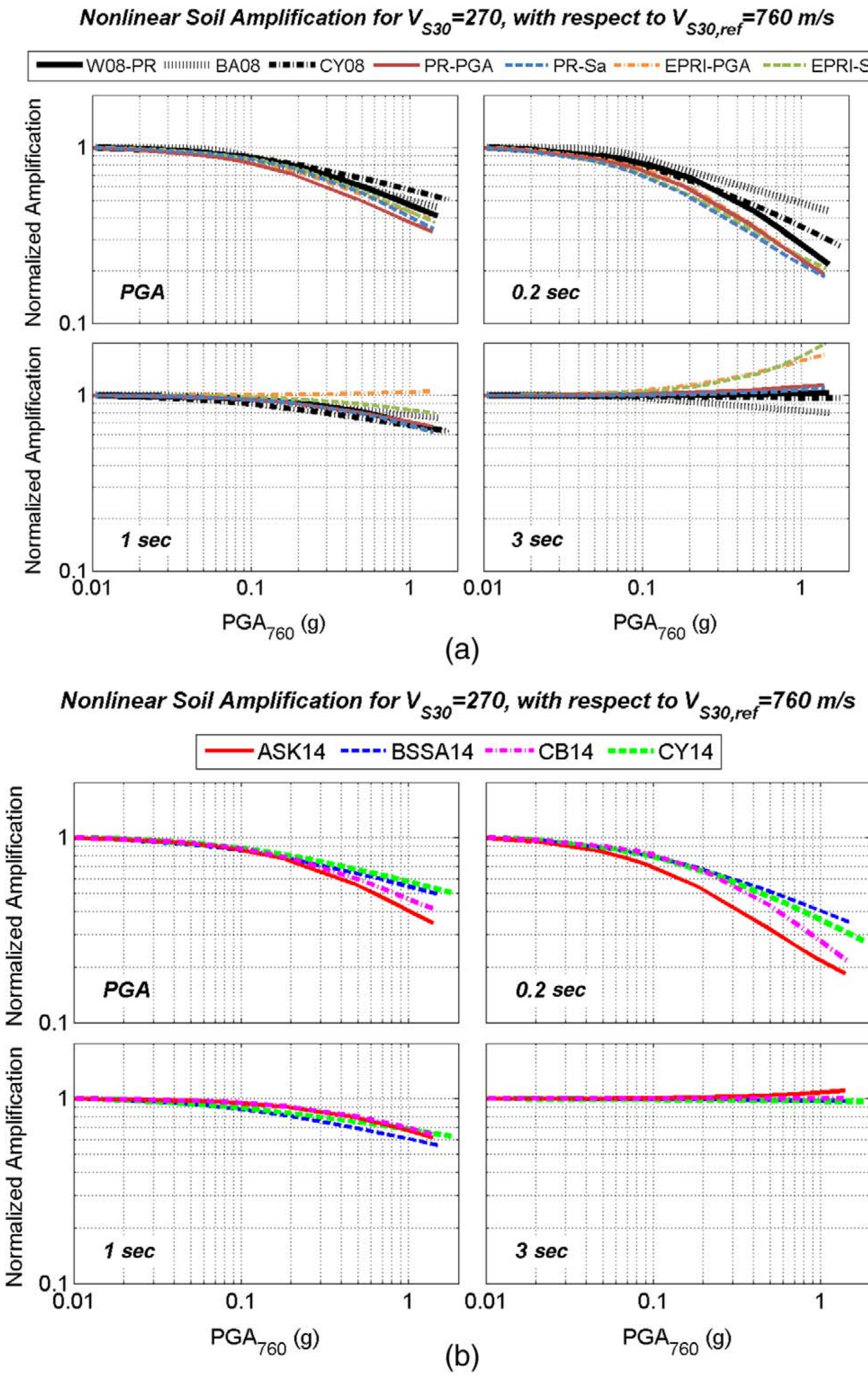

Figure 7. Nonlinear amplification for $V_{S30} = 270$ m/s with respect to $V_{S30,ref} = 760$ m/s, normalized by the amplification at $PGA_{760} = 0.01$ g. (a) Comparing the four proposed models with the other NGA-West1 nonlinear alternatives, and (b) comparing the four NGA-West2 nonlinear models.

such as $T = 0.2$ s. This is partly due to the influence of the new simulated profiles at $V_{S30} =$ 190 m/s (see Figure 4), which were not included in the 2008 simulations.

For sites with a lower V_{S30} (e.g., less than 200 m/s), the same comparison shows less consistency between the models due to lack of data to constrain the data-driven models and due to sensitivity of the simulation-driven models to the choice of soil properties. As previously noted, the GMPE should not replace a site-specific analysis, but the overall nonlinear effects must be incorporated so that the soil data can be included in the development of the full model without biasing magnitude and distance scaling.

Finally, the nonlinear site amplification is compared across the entire period range in Figure 8. In this figure, the nonlinearity is presented in terms of the slope of the lines in Figure 7, between PGA_{1180} of 0.1 g to 1 g, for a profile with $V_{S30} = 270$ m/s. As the curves in Figure 8 deviate from zero, the site response is considered more nonlinear. When the curves in Figure 8 are negative, nonlinearity is expressed by increased damping and deamplification as seen in Figures 5 and 6. When the curves in Figure 8 are positive, nonlinearity is expressed by the softening and period shift, leading to amplification at strong levels of shaking, as seen in Figures 5 and 6. The trends are similar for all four models and are also generally consistent with nonlinearity computed from the Walling models. The nonlinearity for the EPRI models is generally greater than that of the PR models, with the nonlinearity being strongest at periods between $T = 0.15$ s and $T = 0.2$ s for all models.

USE OF EQUIVALENT-LINEAR VERSUS NONLINEAR METHODS

While we acknowledge and recognize the potential shortcomings of the equivalent-linear method to describe nonlinear site response, we believe that it is adequate for our purpose,

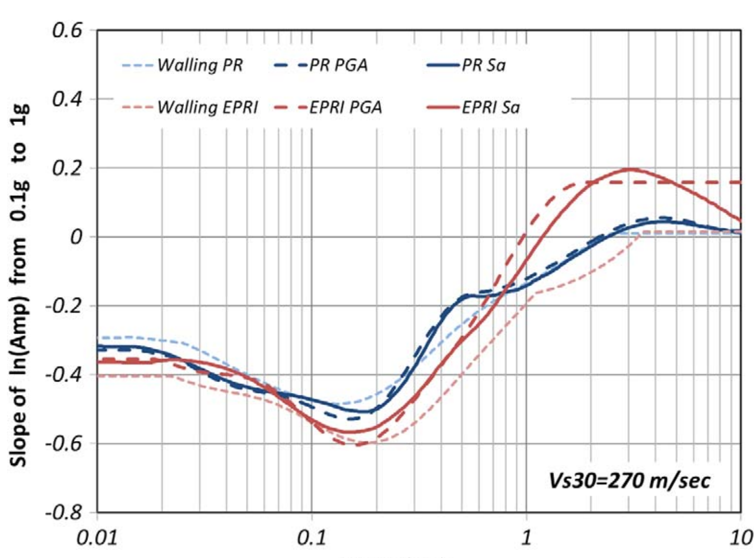

Figure 8. Period-dependence of the combined nonlinear term for soil sites with $V_{S30} = 270$ m/s, computed as the slope of ln(amp) from 0.1 g to 1 g.

which is to provide simple models that would serve as components within an empirical GMPE. As such, the models need to describe the general trends of the nonlinear site response over a very broad range of conditions (soil profiles, depths, input motions, magnitudes) and fit within the framework of the GMPE (in terms of parameter space). As noted previously, our goal is not to create a model that replaces site response, but rather to allow the soil sites to be incorporated into the derivation of a GMPE so that nonlinear soil effects are not mapped into magnitude or distance or hanging wall effects. If the nonlinear response is not included in the GMPE, all soil data must be eliminated, which would greatly reduce the amount of data used at close distances from large earthquakes. While fully time-stepping nonlinear models may be more suitable to describe the site-specific response of single profiles under specific time-histories, equivalent-linear methods have been shown to capture the general response spectra quite satisfactorily for the purpose of generating GMPEs.

PGA VERSUS $Sa(T)$

The predictive power of modeling of the nonlinear site amplification using either PGA_{1180} or $Sa_{1180}(T)$ can be tested by comparing the standard deviation of the simulated ground motions using the two alternative approaches for the strength of shaking. First, the standard deviation of the $\ln(amp)$, referred to here as σ_{amp}, is shown by V_{S30} bins for the two PR models in Figure 9. The average soil σ_{amp}, representing profiles with $V_{S30} \leq 400$ m/s, is shown by the black line. In general, Figure 9 shows that σ_{amp} increases as V_{S30} decreases and that the trends are similar for both the PR-PGA and the PR-Sa models, for all V_{S30} values.

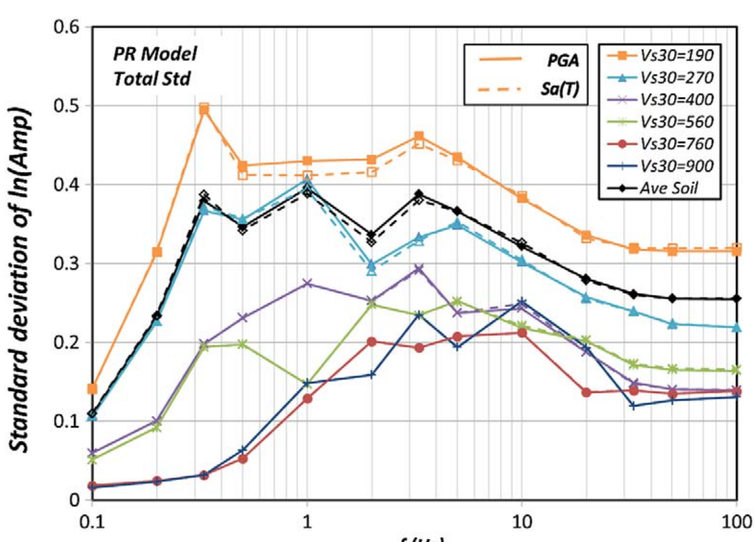

Figure 9. Standard deviation of the PR-PGA model (solid lines) and the PR-Sa model (dashed lines), for a range of V_{S30} values and for the average of all soil profiles ($V_{S30} \leq 400$ m/s).

Figure 10 compares the standard deviation of the site amplification for the two different functional forms (PGA versus Sa as shaking input parameter) for PR soil model, using the average of all soil profiles for comparison. The standard deviations are very similar, indicating that from a statistical basis, the two methods for specifying the level of shaking, PGA_{1180} or $Sa_{1180}(T)$, are similar in their predictive power. These findings are different from the results of Bazzurro and Cornell (2004; denoted as BC04), who concluded that $Sa(T)$ is the single most helpful parameter for the prediction of the amplification since it had the lowest σ_{amp}. A subset of their findings is also shown in Figure 10, comparing the standard deviations of the residuals to two of their functional forms, using PGA and Sa(f) as single model parameters. The velocity profiles presented in Figure 10 are generally comparable—representing the average of two soft soil profiles (with V_{S30} of $200-300$ m/s) in the case of BC04, and the average soil profile in the case of this study, which is almost equal to the $V_{S30} = 270$ m/s profile (see Figure 9). One of the main differences between our simulations and Bazzurro and Cornell's is that they use real time histories that included variability in the spectral shape, whereas the simulations in this study were performed with the random vibration theory (RVT) method, which leads to small variability in the spectral shape (e.g., Figure 11). Uncertainties in soil properties are accounted for in both studies, and do not add to the total uncertainty very much, as long as the general profile (in terms of depth to bedrock and V_{S30}) stays the same.

While our study shows no statistical preference to either of the functional forms, using $Sa_{Ref}(T)$ as the input shaking parameter instead of PGA_{Ref} carries benefits in terms of simpler applicability. Following Al Atik and Abrahamson's (2010) notation, we can describe the spectral amplification on soil as:

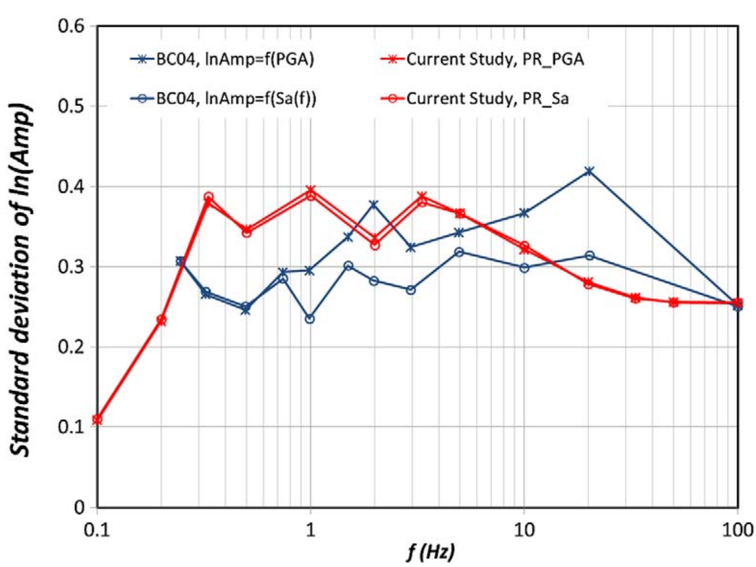

Figure 10. Standard deviation of the site amplification for the two PR models, averaged over all soil profiles ($V_{S30} \leq 400$ m/s). For comparison, a subset of two corresponding models is redrawn from Bazzurro and Cornell (2004), labeled as BC04 in the legend.

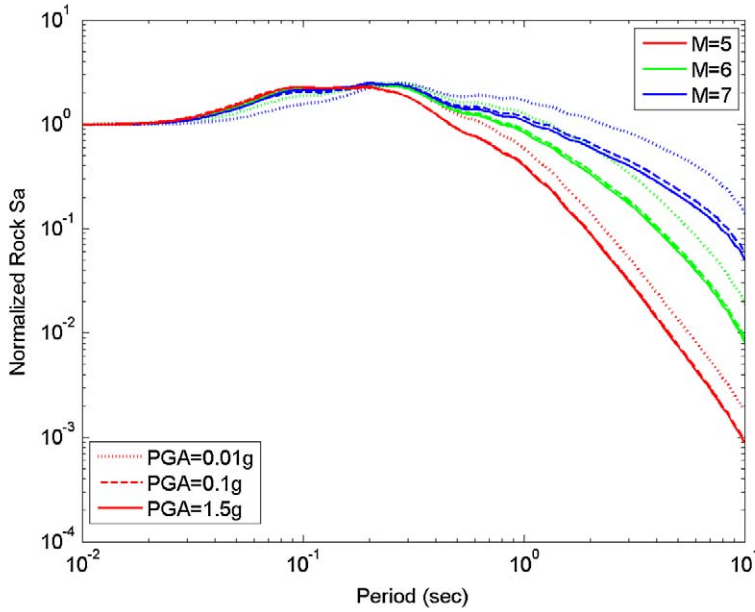

Figure 11. Variability of the input motion spectral shapes: three PGA_{1180} values for each of the three point-source magnitudes. All spectral values are normalized by their PGA value, to represent the shape only.

$$\ln(Sa_{soil}(T)) = \ln(Sa_{Ref}(T)) + \ln Amp(T, V_{S30}, Sa_{Ref}(T_0)) \tag{7}$$

where $T_0 = T$ in the Sa formulation and $T_0 = 0$ in the PGA formation. When $T_0 \neq T$, such as in the PGA formulation, an estimate of both PGA_{1180} and $Sa_{1180}(T)$ is required, accounting for the correlation of the variability between the two parameters. When including the effects of the nonlinear term on the standard deviation, the effect of this additional correlation can be approximated, as shown in Equation 6 in Al Atik and Abrahamson (2010). The *Sa* formulation avoids the need for this approximation and leads to a simpler application.

We conclude that based on the analysis presented herein, and specifically for these models, which are based on the RVT method, there is no statistical preference for either of the forms (PGA or *Sa* as input-motion parameter). Nevertheless, we recommend using the $Sa(T)$ model for ease of use in forward applications of the GMPE model.

SUMMARY

Using a large suite of analytical model results for site amplification, four alternative models to constrain nonlinearity in the new NGA-West2 GMPEs were developed. Although the models are based on a wider simulation data set than that of Walling et al. (2008), the results are generally consistent with the Walling et al. (2008) results for both of the material models considered (PR and EPRI). The reference velocity is redefined as $V_{S30} = 1{,}180$ m/s for better consistency with the simulation procedure, but there should be no effect on the resulting nonlinearity. The main contribution of this study is in deriving the models in terms of either PGA_{1180} or $Sa_{1180}(T)$, to allow the GMPE developers the choice of the parameterization to use. While we show that for the simulations presented in this study there is no statistical benefit to either form, using $Sa(T)$ is easier to use in forward applications of GMPE and thus is recommended.

ACKNOWLEDGMENTS

This study was sponsored by the Pacific Earthquake Engineering Research Center (PEER) and funded by the California Earthquake Authority, California Department of Transportation, and the Pacific Gas & Electric Company. Any opinions, findings, and conclusions or recommendations expressed in this material are those of the authors and do not necessarily reflect those of the above mentioned agencies.

ELECTRONIC SUPPLEMENT

To access the spreadsheet containing the model parameters corresponding to the 111 periods in the NGA-West2 flatfile, please refer to the online edition of this paper.

REFERENCES

Abrahamson, N. A., Atkinson, G. M., Boore, D. M., Bozorgnia, Y., Campbell, K., Chiou, B. S.-J., Idriss, I. M., Silva, W. J., and Youngs, R. R., 2008. Comparisons of the NGA ground motion relations, *Earthquake Spectra* **24**, 45–66.

Abrahamson, N. A., and Silva, W. J., 2008. Summary of the Abrahamson & Silva NGA ground motion relations, *Earthquake Spectra* **24**, 67–97.

Abrahamson, N. A., Silva, W. J., and Kamai, R., 2013. *Update of the AS08 Ground motion Prediction Equations Based on the NGA-West2 Data Set*, PEER Report No. 2013/04, Pacific Earthquake Engineering Research Center, University of California, Berkeley, CA, 143 pp.

Al Atik, L., and Abrahamson, N. A., 2010. Nonlinear site response effects on the standard deviations of predicted ground motions, *Bulletin of the Seismological Society of America* **100**, 1288–1292.

Ancheta, T. D., Darragh, R. B., Stewart, J. P., Seyhan, E., Silva, W. J., Chiou, B. S.-J., Wooddell, K. E., Graves, R. W., Kottke, A. R., Boore, D. M., Kishida, T., and Donahue, J. L., 2014. NGA-West2 database, *Earthquake Spectra* **30**, 989–1005.

Bazzurro, P., and Cornell, C. A., 2004. Nonlinear soil-site effects in probabilistic seismic-hazard analysis, *Bulletin of the Seismological Society of America* **94**, 2110–2123.

Boore, D. M., and Atkinson, G. M., 2008. ground motion prediction equations for the average horizontal component of PGA, PGV, and 5%-damped PSA at spectral periods between 0.01 s 10.0 s, *Earthquake Spectra* **24**, 99–138.

Boore, D. M., Stewart, J. P., Seyhan, E., and Atkinson, G. A., 2014. NGA-West2 equations for predicting PGA, PGV, and 5% damped PSA for shallow crustal earthquakes, *Earthquake Spectra* **30**, 1057–1085.

Campbell, K. W., and Bozorgnia, Y., 2008. NGA ground motion model for the geometric mean horizontal component of PGA, PGV, PGD and 5% damped linear-elastic response spectra for periods ranging from 0.01 and 10.0 s, *Earthquake Spectra* **24**, 139–171.

Campbell, K. W., and Bozorgnia, Y., 2014. NGA-West2 ground motion model for the average horizontal components of PGA, PGV, and 5% damped linear acceleration response spectra, *Earthquake Spectra* **30**, 1087–1115.

Chiou, B. S.-J., Darragh, R., Gregor, N., and Silva, W., 2008. NGA Project Strong-Motion Database, *Earthquake Spectra* **24**, 23–44.

Chiou, B. S.-J., and Youngs, R. R., 2008. An NGA Model for the average horizontal component of peak ground motion and response spectra, *Earthquake Spectra* **24**, 173–215.

Chiou, B. S.-J., and Youngs, R. R., 2014. Update of the Chiou and Youngs NGA model for the average horizontal component of peak ground motion and response spectra, *Earthquake Spectra* **30**, 1117–1153.

Choi, Y., and Stewart, J. P., 2005. Nonlinear site amplification as function of 30 m shear wave velocity, *Earthquake Spectra* **21**, 1–30.

Electric Power Research Institute (EPRI), 1993. *Guidelines for Determining Design Basis Ground Motions*, EPRI TR-102293, Palo Alto, CA.

Idriss, I. M., 2014. An NGA-West2 empirical model for estimating the horizontal spectral values generated by shallow crustal earthquakes, *Earthquake Spectra* **30**, 1155–1177.

Kamai, R., Abrahamson, N. A., and Silva, W. J., 2013. *Nonlinear Horizontal Site Response for the NGA-West2 Project*, PEER Report No. 2013/12, Pacific Earthquake Engineering Research Center, University of California, Berkeley, CA, 69 pp.

Seyhan, E., and Stewart, J. P., 2014. Semi-empirical nonlinear site amplification from NGA-West2 data and simulations, *Earthquake Spectra* **30**, 1241–1256.

Silva, W., and Lee, K., 1987. *WES RASCAL Code for Synthesizing Earthquake Ground Motions*, State-of-the-Art for Assessing Earthquake Hazards in the United States, Report 24, Pacific Engineering and Analysis, El Cerrito, CA.

Silva, W. J, Abrahamson, N. A., Toro, G., and Costantino, C., 1996. *Description and Validation of the Stochastic Ground Motion Model*, Pacific Engineering and Analysis Report, available at http://www.pacificengineering.org/rpts_page1.shtml.

Walling, M., Silva, W. J., and Abrahamson, N. A., 2008. Non-linear site amplification factors for constraining the NGA models, *Earthquake Spectra* **24**, 243–255.

Zhao, J. X., Zhang, J., and Irikura, K., 2009. Side effect of using response spectral amplification ratios for soil sites—variability and earthquake-magnitude and source-distance dependent amplification ratios for soil sites, *Soil Dynamics and Earthquake Engineering* **29**, 1262–1273.

(Received 1 July 2013; accepted 16 December 2013)